

Supplementary information for

A facile evanescent-field imaging approach for monitoring colloidal gel evolution near a surface

Wei Liu,^{a,b,c,d} Jiahao Wu,^d Hui Zhu,^c Chuanxin He,^{*a} and To Ngai^{*d}

^aCollege of Chemistry and Environmental Engineering, Shenzhen University, Shenzhen 518060, China

^bKey Laboratory of Optoelectronic Devices and Systems of Ministry of Education and Guangdong Province, College of Optoelectronic Engineering, Shenzhen University, Shenzhen 518060, China

^cCollege of Food Engineering and Biotechnology, Hanshan Normal University, Chaozhou 521041, China

^dDepartment of Chemistry, The Chinese University of Hong Kong, Shatin, N.T., Hong Kong, China

*Corresponding Authors: Hecx@szu.edu.cn; tongai@cuhk.edu.hk

Materials. *N*-isopropylacrylamide (NIPAM) was recrystallized in a benzene/*n*-hexane mixture. *N,N'*-Methylenebis(acrylamide) (BIS) was recrystallized in methanol. Potassium persulfate (KPS) and sodium dodecyl sulfate (SDS) were used as received. All chemicals were purchased from Sigma-Aldrich, US as analytical reagent.

Microgel Synthesis. PNIPAM microgels were synthesized via a standard one-pot precipitation polymerization.¹ NIPAM (8.09 g), BIS (0.58 g), and SDS (0.29 g) were dissolved in 295 mL MilliQ water and put into a flask with a magnetic stirrer, a reflux condenser, and a nitrogen gas inlet. After the solution was stirred for 40 min at 70 °C under nitrogen, KSP (0.27 g)/5 mL MilliQ water was injected to initiate the polymerization. The reaction was maintained at 70 °C for 4 hours. To remove unreacted chemicals and surfactants, the dispersion was purified via filtration (0.45 μm Nylon filter membranes, Sigma-Aldrich, US) and dialysis (50 kDa MWCO, Spectra/Por Labs, CA) for 4 days. The dispersion was concentrated to 0.0554 g/mL by rotary evaporation.

Characterizations. The hydrodynamic diameter D_h of the microgels was determined by dynamic light scattering (ALV/DLS/SLS-5022F, correlator ALV5000, $\lambda = 632.8$ nm) at $c = 4.3 \times 10^{-7}$ w/w. The DLS data corresponded to the intensity autocorrelations at scattering angles from 20° to 40°, each

measurement was acquired over 300 seconds. The solution was allowed to equilibrate at least for 1 hour at each temperature before measurement.

The intrinsic viscosity $[\eta]$ of the microgel dispersions was measured through a Cannon-Ubbelohde viscometer (No. 25-B164, Cannon Instrument Co., US) at $c = 2\text{--}10$ mg/mL. The effective volume fraction ϕ_{eff} of the microgels was estimated by $\phi_{\text{eff}} = bcD_h^3/2.5$, where b is the proportionality constant between $[\eta]$ and D_h^3 based on the Huggins and Mead–Fuoss plots.²⁻⁴

The zeta potential ζ of the microgels was determined via a Zetasizer Nano (ZS90, Malvern Instruments Inc., UK) at $c = 5.5 \times 10^{-5}$ w/w. The measurement was conducted three times at set temperatures with an equilibration time ≥ 5 min. ζ is presented as the mean \pm standard deviation.

The penetration depth d_p was estimated by $d_p = \lambda/[4\pi\sqrt{(n_1\sin\theta)^2 - n_2^2}]$, where $\lambda = 632.8$ nm is the laser wavelength, $\theta = 70^\circ$ is the incident angle, $n_1 = 1.52$ is the refractive index of the 70° prism, and $n_2 \approx 1.35$ is the refractive index of the dispersion at $c = 0.0554$ g/mL at temperatures from ~ 35 °C to 40 °C, which was measured by an Abbe refractometer (Model 102539, 2WA-J, Shanghai, CN).

Instrumental setup. The microgel dispersion was injected into an ultrathin flow cell ($200 \mu\text{m}$ inner thickness, hollow rectangular capillaries, Borosilicate Glass Co., US), placed on a homemade thermal control device (see Fig. S2) including a recirculating water bath (THX-05, Ningbo Tianheng Instrument Co., CN), two Peltier modules (TEC1-06306, Hebei I.T. (Shanghai) Co. Ltd., CN), and a PID controller with three negative temperature coefficient (NTC) sensors (PR-59, Laird Technologies Inc., US). For each measurement, the temperature was increased from room temperature (~ 25 °C) to a set one at a rate of ~ 0.1 °C/min. Once the set temperature is reached, the images were recorded for 10 s at $t = 0$ s, 300 s, 600 s, and 1200 s, respectively.

The thermal control device was equipped on an inverted Leica DM LFSA microscope with a $50\times$ objective (N PLAN, NA = 0.5, WD = 7 mm). An evanescent field was generated by a laser beam with a wavelength of 632.8 nm at the glass/liquid interface where the penetration depth d_p is ~ 110 nm. The scattering images were captured by a sCMOS camera (Zyla 5.5, 2560×2160 pixels, pixel size = $6.5 \mu\text{m}$, Andor Technology Ltd., UK) at a sampling rate of 10–50 fps. More details could be found in Fig. S2.

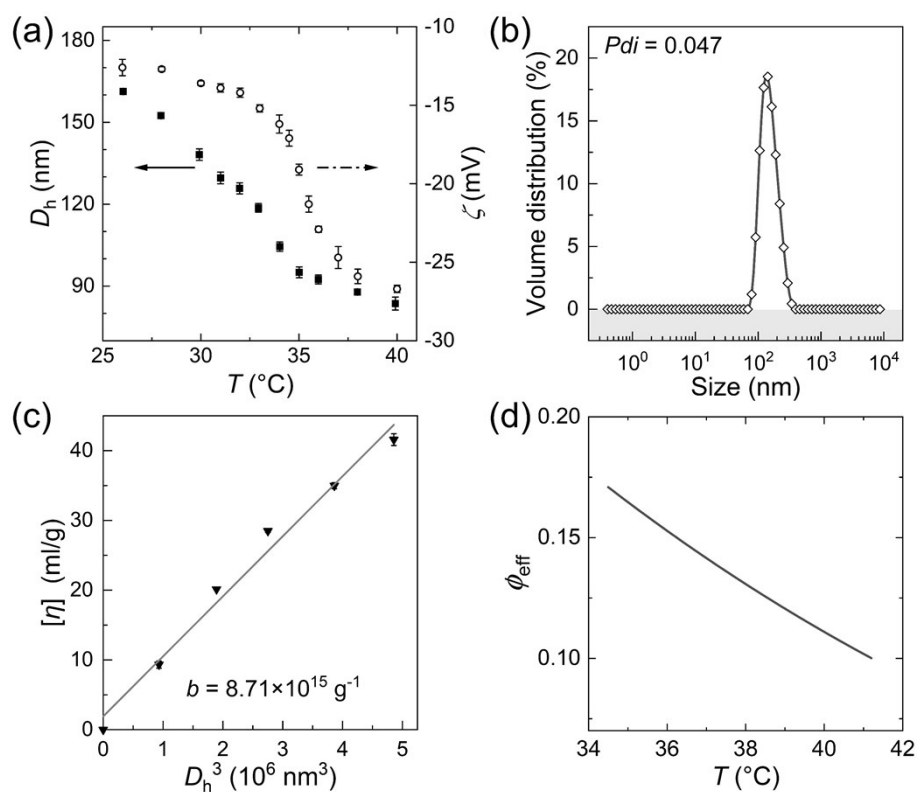


Fig. S1 (a) The hydrodynamic diameter D_h (squares) and zeta potential ζ (circles) of PNIPAM microgels as a function of temperature. (b) Typical particle size distribution of microgels at 25 °C. The polydispersity index (Pdi) < 0.05. (c) The intrinsic viscosity $[\eta]$ of microgel dispersions as a function of D_h^3 . (d) The effective volume fraction ϕ_{eff} of microgels as a function of temperature.

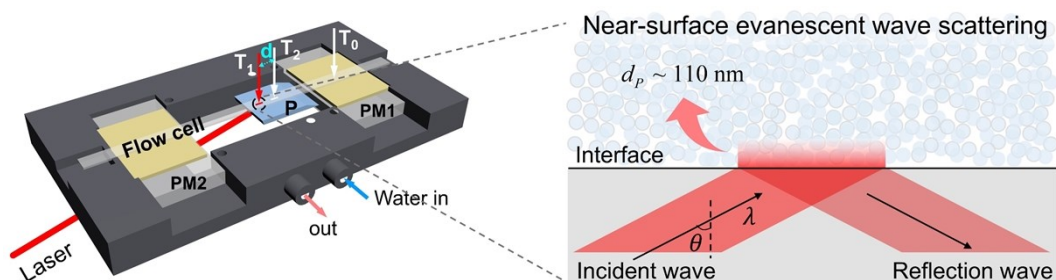


Fig. S2 Schematic of the thermal control device incorporated on a total internal reflection microscope (TIRM). P is the 70° prism, PM1 and PM2 are the Peltier modules and/or copper plates (yellow). T_0 , T_1 , and T_2 are temperatures at individual regions along the flow cell. d (~5 mm) is the distance between regions T_1 and T_2 . At region T_1 , an evanescent field is generated on the liquid/glass interface with $d_p \sim 110$ nm, where the scattering intensity is recorded by a sCMOS camera.

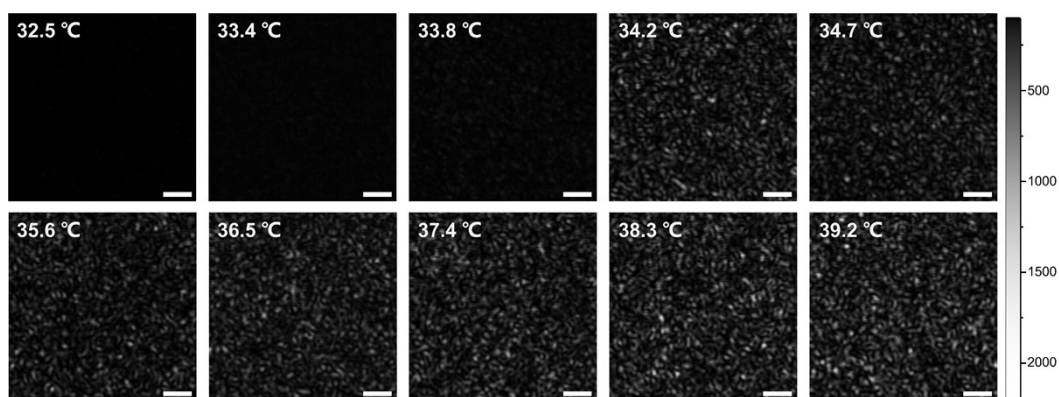


Fig. S3 Original total internal reflection microscope (TIRM) images of colloidal gels. The dynamic speckles emerge after 34 °C, corresponding to $\phi_{\text{eff}} \sim 0.23$. Scale bars represent 5 μm . Gray scale represents the intensity.

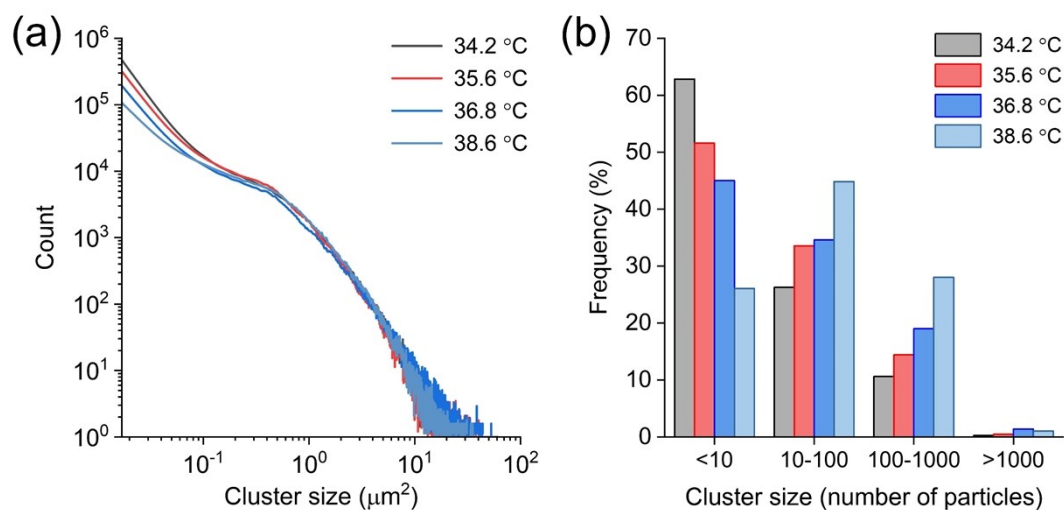


Fig. S4 Cluster size distribution in count (a) and histogram (b) at different temperatures. The clusters are 2D projections, which sizes are counted based on a sequence of binarized images after default thresholding via *ImageJ*.

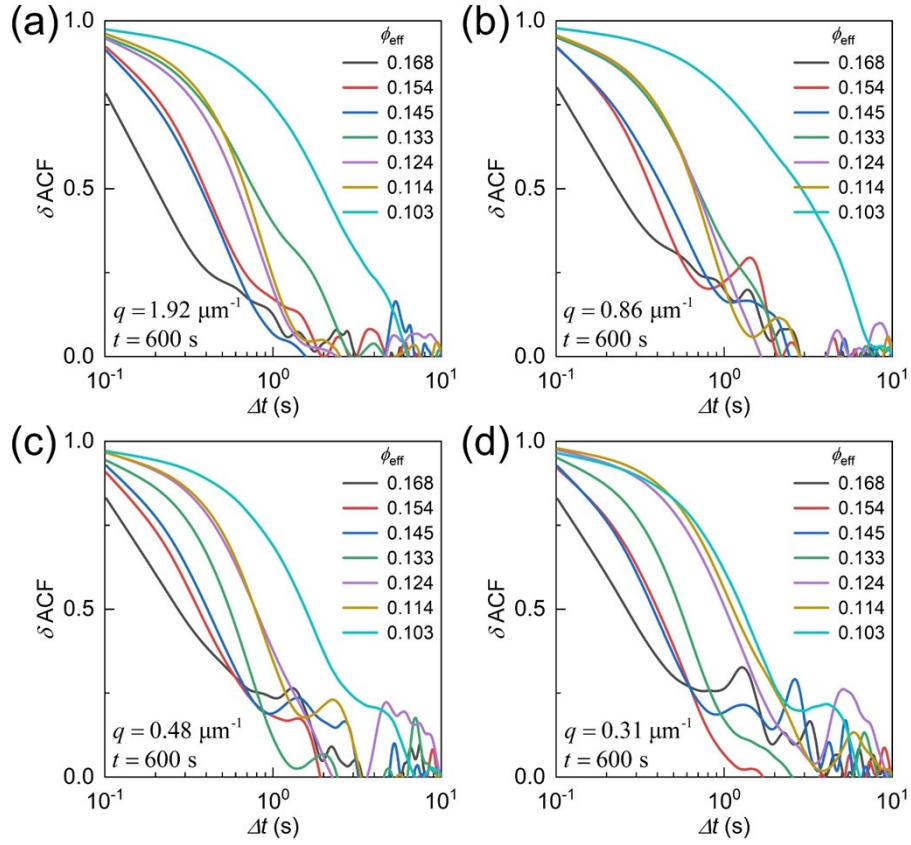


Fig. S5 Typical density-fluctuation autocorrelation functions (δACF) for ϕ_{eff} varying from 0.103 to 0.168 at various q from $0.31 \mu\text{m}^{-1}$ to $1.92 \mu\text{m}^{-1}$ ($t = 600 \text{ s}$).

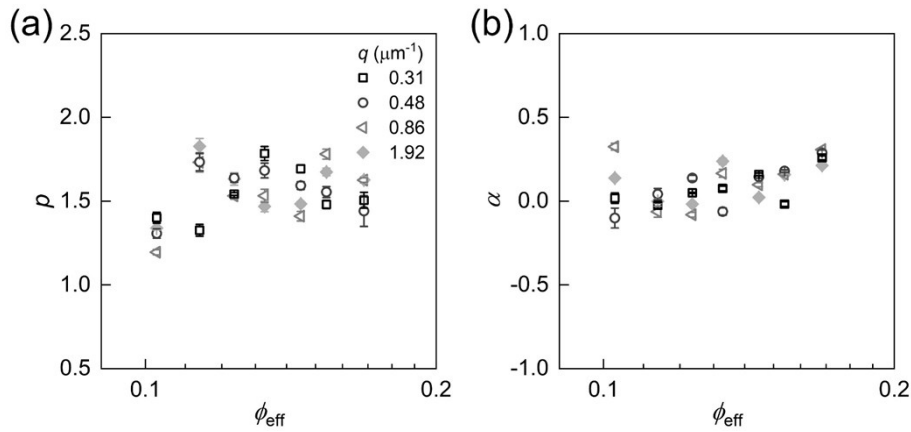


Fig. S6 Fitting parameters p and α for the compressed exponential decay functions at different ϕ_{eff} at various q from $0.31 \mu\text{m}^{-1}$ to $1.92 \mu\text{m}^{-1}$ ($t = 600 \text{ s}$).

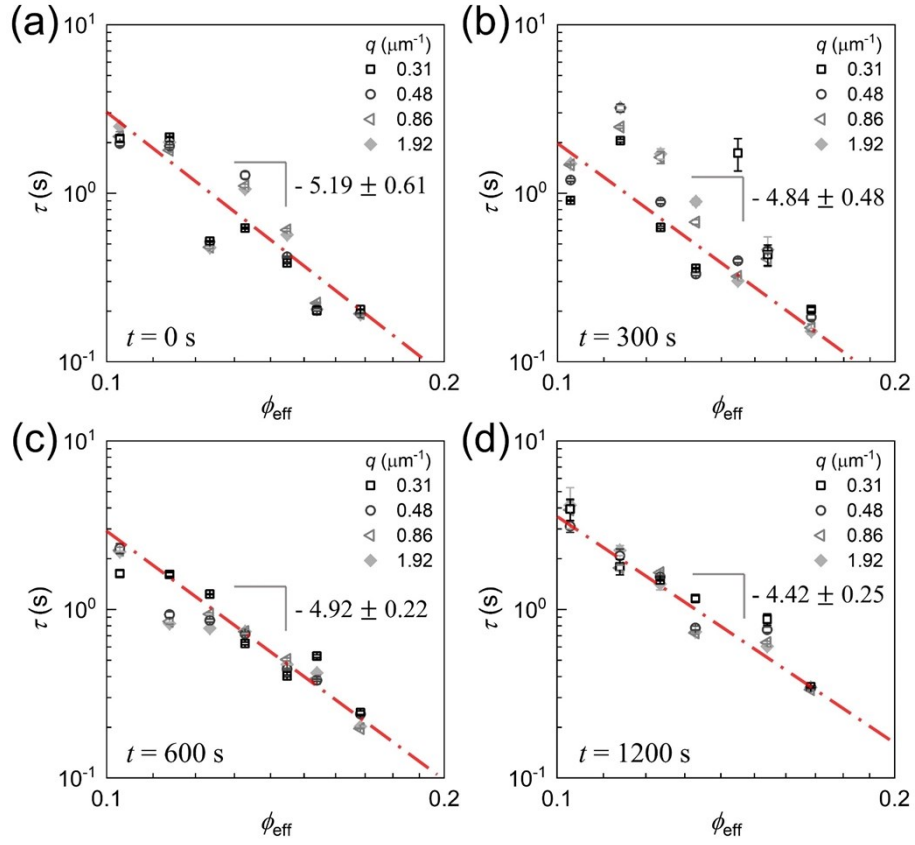


Fig. S7 Relaxation time τ as a function of ϕ_{eff} at various q from $0.31 \mu\text{m}^{-1}$ to $1.92 \mu\text{m}^{-1}$ at $t = 0$ s (a), 300 s (b), 600 s (c), and 1200 s (d). The dash-dotted lines represent the linear fitting.

References

1. Y. Zhao, Y. Cao, Y. L. Yang and C. Wu, *Macromolecules*, 2003, **36**, 855-859.
2. T. Kureha, H. Minato, D. Suzuki, K. Urayama and M. Shibayama, *Soft Matter*, 2019, **15**, 5390-5399.
3. S. Minami, T. Watanabe, D. Suzuki and K. Urayama, *Soft Matter*, 2018, **14**, 1596-1607.
4. A. Omari, R. Tabary, D. Rousseau, F. L. Calderon, J. Monteil and G. Chauveteau, *J. Colloid Interface Sci.*, 2006, **302**, 537-546.